

## 5. Kinetic Simulation of Micro Plasmas

YANG Sung Soo, KIM Sung Jin and LEE Jae Koo\*

*Department of Electronic and Electrical Engineering,  
Pohang University of Science and Technology (POSTECH), Pohang, 790-784, Korea.*

(Received 20 October 2003)

### Abstract:

Kinetic simulation is a good numerical method for investigating plasma characteristics and behavior in a collisional micro plasma display because the kinetic simulation code describes the motion of particles with relatively better accuracy than that of the fluid simulation code. Using two-dimensional kinetic simulation code, we calculated the ion incident angle and energy distributions on the dielectric surface of the cathode region in an alternating-current plasma display panel cell with variations in gas mixture, cell type, and pressure. The angle distribution of ions impinging on the cathode surface is one of the important factors for accurate experimental measurement of the secondary electron emission coefficient and for estimation of MgO sputtering. We also observed the striation phenomenon in a PDP cell and attempted to explain the striation mechanism based on the kinetic simulation results.

### Keywords:

numerical simulation, kinetic code, gas discharge, plasma display panel, striation

### 5.1 Introduction

The alternating current plasma display panels (AC-PDPs) are the leading flat panel display devices to realize the digital high-definition (HD) TV with diagonal over 70 inches [1]. Although PDPs have more advantages than other displays in aspects of screen size, thickness, weight, and wide view angle, low luminous efficiency is still one of the most important issues in PDP research. To improve the luminous efficiency, it is necessary to investigate the plasma discharge behavior and characteristics in a PDP cell.

The principle of a PDP cell is similar to that of an ordinary household fluorescent lamp. PDPs use ultra-violet (UV) emitted from gas discharge and the phosphor to convert UV to visible photons. The detailed principle and structure of a PDP cell are described in Ref. 1. Some experiments presented useful information on discharge behavior from the measurement of UV or infrared (IR) emission. However, the experimental access to plasma discharge has limitations due to the small cell size (a few hundred mm) and short discharge time (1~2  $\mu$ s). Therefore, numerical simulation is a very useful method for investigating the plasma discharge. Generally, for the PDP simulation, fluid and kinetic codes are used. We have developed 2-D and 3-D fluid simulation code for a PDP cell with radiation transport model [2-5]. Using the fluid code, we can obtain various data such as spatio-temporally resolved plasma density, potential, electric field, and wall charge distributions. In addition, luminance and efficiency can be also obtained from the calculation of UV

emission. Therefore, we can diagnose the discharge characteristics quickly and suggest new cell designs with high luminous efficiency [6]. For a more accurate modeling, we should also consider the kinetic effects. The kinetic code (XOOPIC [7]) describes the motion of particles and does not make any assumptions. It provides more accuracy in numerical calculation in comparison with the fluid code. As the kinetic code gives the velocity information of particles, the angle and energy distributions of particles in a PDP cell can be calculated.

In this paper, we explain the advantage of kinetic code and present several kinetic simulation results in PDP research. We introduce the method of kinetic code and simulation conditions for PDP research in Sec. 5.2. In Sec. 5.3.1, the striation phenomenon in a microdischarge system and its mechanism are described briefly. In Sec. 5.3.2, simulation results for ion incident angle and energy distributions by kinetic code are given. Finally, we summarize our work in Sec. 5.4.

### 5.2 Simulation Condition

#### 5.2.1 Method of PIC-MCC simulation

Plasma simulation, Particle-in-Cell (PIC) merged with Monte-Carlo collision (MCC) including null collision method, is widely used to understand complex plasma theory and application to partially ionized gases. Changes in charged particle speed and direction due to collision with neutrals, including elastic, excitation, ionization, charge exchange and

\*corresponding author's e-mail: jkl@postech.ac.kr

attachment process, are considered by using MCC method [8,9]. Computer particles called super-particles are assigned to reduce real simulation time. Super-particles represent many real particles.

Figure 1 shows a computing sequence for the PIC-MCC simulation. Many super-particles are loaded in meshes [8,9]. They are weighted in grids by using various weighting methods. In general, nearest-grid point (zero-order weighting) is applied to 1-D simulation. Piecewise linear (first-order weighting) or piecewise parabola (second-order weighting) is used in 2-D and 3-D codes. For electrostatic case, electric field and potential are obtained from the following Poisson's equation :

$$\nabla^2 V = -\frac{\rho}{\epsilon_0}.$$

Position and velocity of particles are calculated as follows,

$$\vec{F} = q(\vec{E} + \vec{V} \times \vec{B}) = m \frac{d\vec{v}}{dt}, \quad \frac{d\vec{x}}{dt} = \vec{v}.$$

For electromagnetic case, Maxwell's equations are used. Collisions between charged particle and neutral are calculated by MCC. Collisional probability is calculated by

$$P_i = 1 - \exp[-\Delta t v_i \sigma_T(\epsilon_i) n_i(x_i)],$$

where  $n_i(x_i)$  is the local density of the target species at the position of particle. As a computed random number ( $R$ ) is compared with collision probability, it is confirmed whether collision takes place ( $R < P_i$ ) or not [9]. These steps are repeated as shown in Fig 1.

### 5.2.2 Simulation domain and conditions for PDP

For many other low-temperature plasma researches, PIC-MCC simulation has been used [10-13]. For PDP simulation with 2-D kinetic code, we use typical coplanar- and matrix-type AC-PDP geometries presented in Figs. 2(a) and (b), respectively. A coplanar-type PDP cell has two sustain electrodes (anode and cathode) on the same dielectric layer. The cell width and height are 1,260  $\mu\text{m}$  and 210  $\mu\text{m}$ , respectively. The gap distance  $d$  between two sustain electrodes is 60  $\mu\text{m}$  and the length  $l$  of each sustain electrode is 400  $\mu\text{m}$ . The secondary electron emission coefficient for Ne and Xe ions on upper dielectric layer are assumed to be 0.5 and 0.05, respectively. In case of a matrix-type PDP cell, because one electrode is opposite to the other as presented in Fig. 3(b), the main discharge occurs vertically. Therefore, a matrix-type PDP cell has major problems in stability and lifetime of the phosphor since the phosphor is bombarded by the charged particles from the discharge.

Generally, to operate AC-PDP cell, many square pulses with 50 kHz ~ 100 kHz are applied to the two sustain electrodes alternately. However, since we started kinetic simulation without pre-accumulated surface charges, we needed a large driving voltage compared to the general sustain voltage (about 200 V). Therefore, in these simulations, we

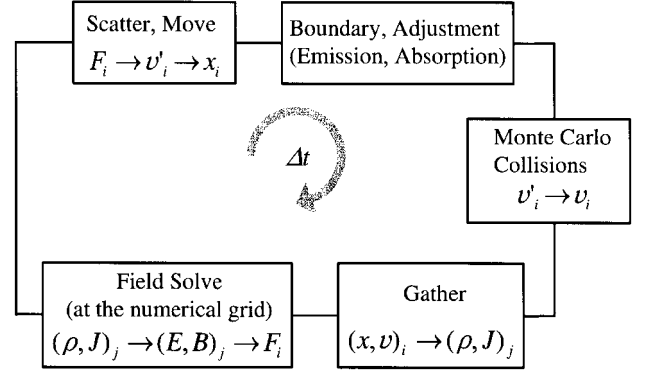


Fig. 1 Computing sequence for MCC-PIC simulation (Ref. [9]).

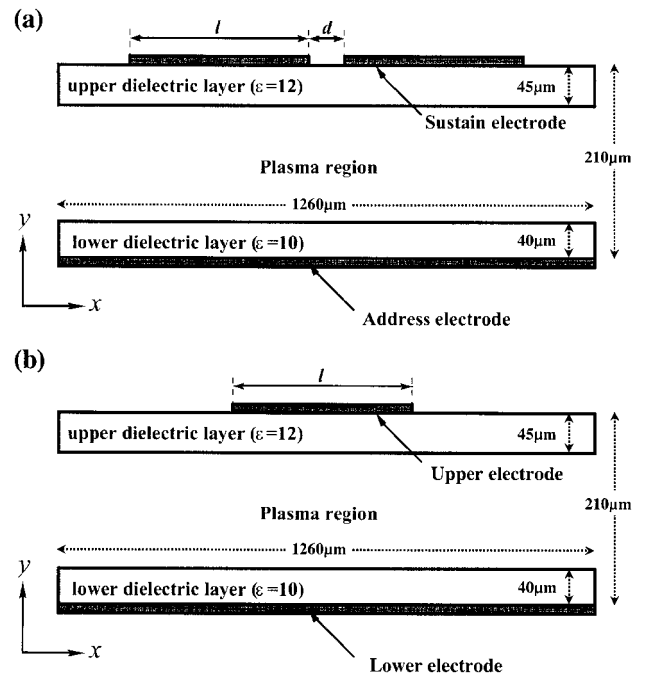


Fig. 2 Schematic diagram of the (a) coplanar-type AC-PDP cell and (b) matrix-type AC-PDP cell for 2-D kinetic simulation. The gap distance  $d$  is 60  $\mu\text{m}$  and the electrode length  $l$  is 400  $\mu\text{m}$ .

applied driving voltages with 350 V, 0 V, and 175 V for the anode, the cathode and the address electrode, respectively. The rising and falling time of driving pulses are 200 ns. As these kinetic simulations need very long simulation time, we simulated only one pulse period. To investigate the dependence on gas pressure and gas composition, we have carried out simulations for different gas pressures, and several different Xe concentrations on Ne based gas.

The simulation conditions are as follows. The initial densities of the kinetic simulation are  $10^{16}/\text{m}^3$  for electrons and ions, and each super particle represents actual particles of  $10^6$ . Therefore, initial simulation particle numbers of electrons and positive ions are 1574 in a cell and these particles are distributed with uniformity in plasma region as shown in Fig. 2. The simulation time step is  $2.0 \times 10^{-13}$

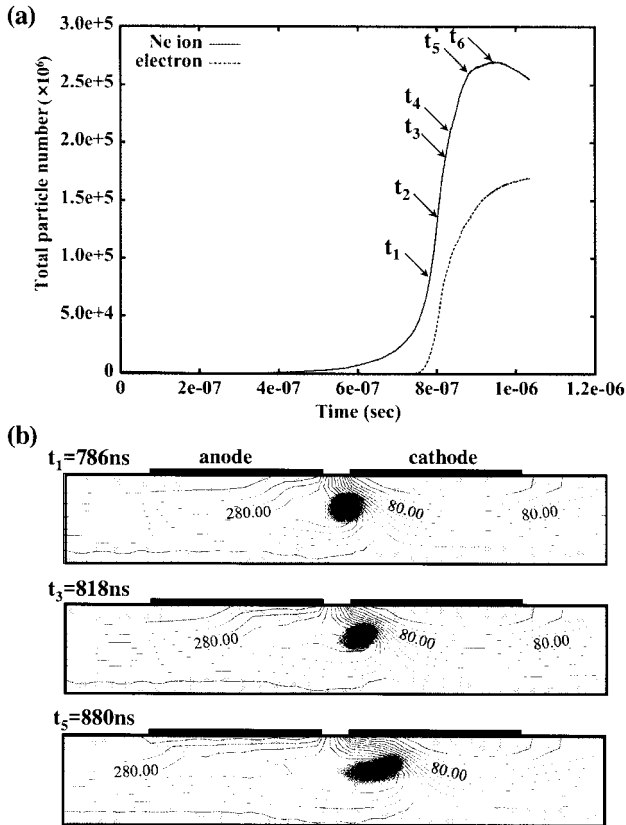


Fig. 3 (a) Time traces of plasma particle numbers and (b) series of Ne ion density distribution with potential profile at three observation points ( $t_1$ ,  $t_3$ , and  $t_5$ ) in a coplanar-type PDP cell. The striation can be observed at the anode region.

second.

## 5.3 Simulation Results

### 5.3.1 Striation phenomena

Some experiments reported the several locally discrete peaks in the anode region of PDP cell through the observation of visible light or IR emission. This is the striation phenomena on AC-PDP anode surface. The striation is due to the localized charged and excited species density humps on the anode region. We have described the self-consistent mechanism of the striation in a coplanar-type AC-PDP cell based on various kinetic simulation diagnostics [14]. In the kinetic simulations with pure Ne, gas pressure of 500 Torr, and the several parameters described in Sec. 5.2.2, the striation phenomenon is clearly observed as shown on a coplanar-type AC-PDP cell. Figure 3(a) is the time traces of plasma particle numbers and Fig. 3(b) is the series of Ne ion density distribution with potential profile at three observation points ( $t_1$ ,  $t_3$ , and  $t_5$ ) indicated in Fig. 3(a). Wide density hump is located near the inner edge of the anode. It gets extended toward the cathode as time goes on. The other small density humps are shown one by one sequentially toward the outer edge of the anode in alignment along the dielectric surface. The generation of small density hump is stopped at the end of the electrode.

The discharge mechanism near the anode surface is ionization by energetic electrons. The accumulated negative surface charges by electrons diminished the applied potential on the anode dielectric locally. The changed potential makes another channel for energetic electrons to produce the next plasma density hump and prevents the movement of previously developed plasma ions. In the simulation of a matrix-type AC-PDP cell, the striation is also observed on the anode side. We can also observe the striation in fluid simulation. However, the striation is not clear in fluid simulation because the localization of the density humps is not strong enough and the humps smear out faster than that of kinetic simulation.

### 5.3.2 Ion angle and energy distributions

The secondary electron emission coefficient ( $\gamma_{se}$ ) of protecting layer is an essential parameter for determining driving voltage range and for understanding the discharge mechanism in a PDP cell. There have been many experiments and theoretical approaches to find the value of  $\gamma_{se}$  for MgO or other protective materials. However, different  $\gamma_{se}$  values have been obtained in these experiments and theoretical works. Generally, in experiment, ion beam is used to measure the  $\gamma_{se}$  value from the target materials. However, the energies of the ion beam in most experiments are much higher than ion energies calculated at the cathode region in our kinetic simulation [15]. In addition, ion beam is directed perpendicular to the target material surface. Ion incident angle, which means the angle from the surface normal, is also a very important factor for sputtering. In PDP system, gas pressure is very high and charge exchange collisions between ions and neutrals occur frequently at the sheath region of the cathode. As a result, ions at the cathode region cannot have high energy compared to the sheath voltage drop. Because a coplanar-type PDP cell has two sustain electrodes on the same dielectric layer unlike a matrix-type PDP cell, we estimated the incident angles of ions impinging on the MgO surface to be higher than  $0^\circ$ . Unfortunately, the observation of incident angles in a real PDP cell is not easy. Therefore we have investigated the incident angle and energy distributions of ions on the cathode surface using the kinetic simulation code.

To compare the ion angle distributions on the cathode surface for coplanar-type and matrix-type PDP cells, we simulated these two types of PDP cell with pure Ne gas and gas pressure of 500 Torr. While the ion incident angle for the largest particle number of a matrix-type PDP cell is around  $4^\circ$ , that of a coplanar-type PDP cell is around  $18^\circ$  and 90% of Ne ions at the MgO surface have the incident angles in the range of  $6^\circ \sim 30^\circ$  as shown in Fig. 4. In case of a matrix-type PDP cell, the cathode is opposite to the anode, and the direction of the electric field at the cathode sheath region is close to the normal on the MgO surface.

We also carried out the simulation for Ne-Xe mixture case with gas pressure of 500 Torr in a coplanar-type PDP cell using the several parameters described in Sec. 5.2.2. Figure 5 shows the incident angle distributions of Ne ions and Xe ions with 10% Xe concentration. The incident particle numbers are integrated until the total number of Xe ions in a

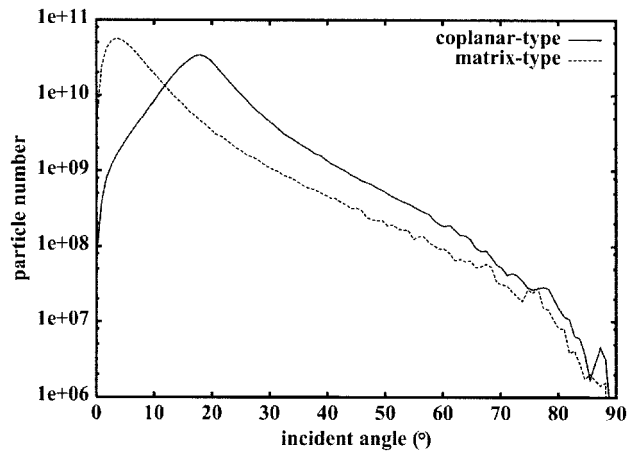


Fig. 4 Comparison of incident ion angle distributions on the cathode surface between matrix-type and coplanar-type PDP cells. For this simulation, Ne 100% gas with 500 Torr is used. Particle numbers are integrated until the total number of Ne ions in a cell space reaches the maximum.

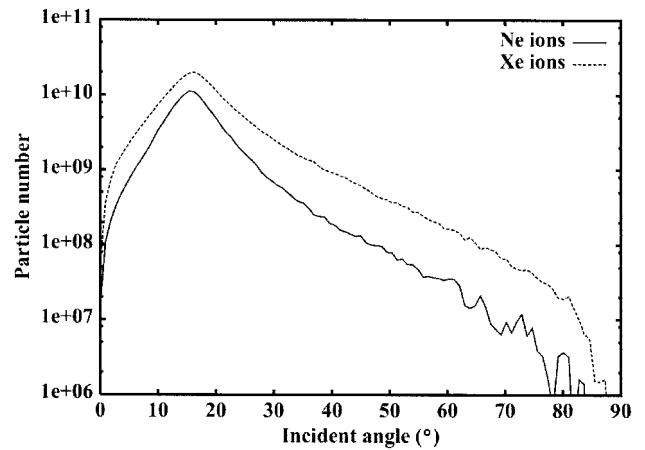


Fig. 5 Incident angle distributions of Ne and Xe ions on the cathode surface with the condition of Xe(10%)-Ne (90%) and 500 Torr in a coplanar-type PDP cell. Particle numbers are integrated until the total number of Xe ions in a cell space reaches the maximum.

cell space reaches the maximum. Since the collision cross section for ionization of Xe is larger than that of Ne, a large number of Xe ions are produced and arrive at the MgO surface of the cathode region. Ne and Xe ions have the similar incident angles for the largest particle number in the range of  $15^{\circ}\sim 16^{\circ}$ . These angles are smaller than the case of pure Ne. To observe the dependence of Xe concentration, we simulated several cases of Xe concentration (4%, 10%, and 20%). The ion incident angle for the largest particle number increases slightly. However, there is no noticeable variation in the incident angle distributions. The incident angle of new ions generated by charge exchange collisions in the cathode sheath region seems to be influenced dominantly by the direction of the electric field at the cathode sheath rather than by total gas pressure or Xe concentration.

To observe the pressure dependence in a coplanar-type PDP cell, we simulated for three different values of pressures (400, 500, and 600 Torr) for the same time duration using Xe 10%-Ne 90% mixture gas with several parameters described in Sec. 5.2.2. The Xe ion incident angles increased slightly with the increase in gas pressure. However, Xe ions cannot have high energies as the total pressure increases as presented in Fig. 6. The mean free path of ions is inversely proportional to gas pressure. As total pressure in a PDP system is around a few hundred Torr, the mean free path of ions is less than  $1\ \mu\text{m}$  and charge exchange collisions between ions and neutrals occur frequently at the cathode sheath region. New ions generated by charge exchange collision are accelerated through remainder of the sheath. Therefore the ion energy obtained from the sheath region becomes lower as the number of collisions increases.

## 5.4 Summary

Using the 2-D kinetic code, we observed the striation phenomenon and described its mechanism in a

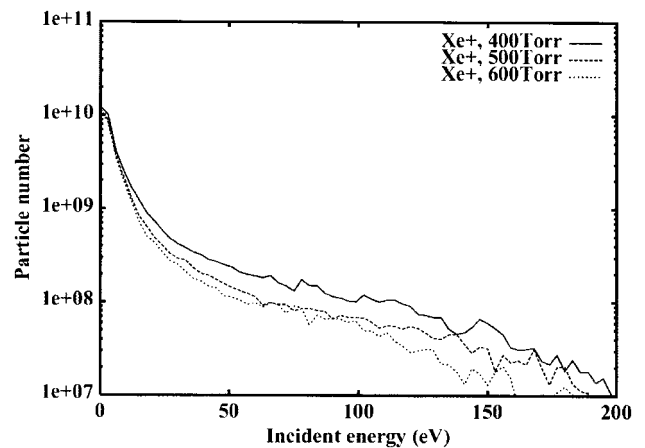


Fig. 6 Comparison of incident Xe ion energy distributions on the cathode surface with three different gas pressures (400, 500, and 600 Torr) and Xe(10%)-Ne(90%) mixture gas in a coplanar-type PDP cell. Particle numbers are integrated during 20 ns after the total number of Xe ions in a cell space reaches the maximum.

microdischarge system such as coplanar- and matrix-type AC-PDP. The striation phenomenon is associated with the dielectric charge accumulation affecting the potential distribution near the anode. We also found that most ions impinging on the MgO layer at the cathode dielectric in a coplanar-type PDP cell have incident angles larger than  $0^{\circ}$  with respect to the normal to the surface in pure Ne and Ne-Xe mixed gases at 400~600 Torr. The incident ion angle distribution shows the way to obtain more accurate  $\gamma_{se}$  values in experiment. In a matrix-type PDP cell, incident angles for the largest particle number are about  $4^{\circ}\sim 5^{\circ}$  and 90% ions have the incident angles in the range of  $0^{\circ}\sim 16^{\circ}$ . However, in a coplanar-type PDP cell, incident angles for the largest particle number are in the range of  $15^{\circ}\sim 20^{\circ}$ .

## Acknowledgment

The authors would like to thank N. Babaeva, and C.H. Shon for their helpful discussions.

## References

- [1] J.K. Lee and J.P. Verboncoeur, *Low Temperature Plasma Physics*, ed. by R. Hippler *et al.*, (Wiley-VCH, Berlin, Germany, 2001) p. 367.
- [2] Y.K. Shin, C.H. Shon, W. Kim and J.K. Lee, *IEEE Trans. Plasma Sci.* **27**, 1366 (1999).
- [3] H.C. Kim, M.S. Hur, S.S. Yang, S.W. Shin and J.K. Lee, *J. Appl. Phys.* **91**, 9513 (2002).
- [4] H.J. Lee, H.C. Kim, S.S. Yang and J.K. Lee, *Phys. Plasmas* **9**, 2822 (2002).
- [5] H.C. Kim, S.S. Yang and J.K. Lee, *J. Appl. Phys.* **93**, 9516 (2003).
- [6] S.S. Yang, H.C. Kim, S.W. Ko and J.K. Lee, *IEEE Trans. Plasma Sci.* **31**, 596 (2003).
- [7] J.P. Verboncoeur, A.B. Langdon and N.T. Gladd, *Compt. Phys. Commun.* **87**, 199 (1995).
- [8] C.K. Birdsall, *IEEE Trans. Plasma Sci.* **19**(2), 65 (1991).
- [9] V. Vahedi and M. Surendra, *Compt. Phys. Commun.* **87**, 179 (1995).
- [10] C.H. Shon and J.K. Lee, *Advances in Low Temperature RF Plasmas*, ed. by T. Makabe, (Elsevier Science B.V., Netherlands, 2002) p. 258.
- [11] S. Yonemura and K. Nanbu, *IEEE Trans. Plasma Sci.* **31**, 479 (2003)
- [12] S.J. You, H.C. Kim, C.W. Chung, H.Y. Chang and J.K. Lee, *J. Appl. Phys.* **94**, 7422 (2003).
- [13] G. Wakayama and K. Nanbu, *IEEE Trans. Plasma Sci.* **31**, 638 (2003).
- [14] C.H. Shon and J.K. Lee, *Phys. Plasmas* **8**, 1070 (2001).
- [15] Y.K. Shin, J.K. Lee, C.H. Shon and W. Kim, *Jpn. J. Appl. Phys.* **38**, L174 (1999).